Optical Properties and Local Structure of Eu^{3+} Ions in Sol−Gel TiO_2−SiO_2 Glasses

Hongpeng You and Masayuki Nogami*

Department of Materials Science and Engineering, Nagoya Institute of Technology, Showa, Nagoya 466-8555, Japan

Received: March 29, 2004; In Final Form: June 1, 2004

TiO_2−SiO_2 glasses containing Eu^{3+} ions have been prepared by the sol−gel method. The energy transfer from the O−Ti charge-transfer band to the Eu^{3+} ions was observed. The intensity ratio of $^5D_0 \rightarrow {}^7F_2$ to $^5D_0 \rightarrow {}^7F_1$ increases and the spectrum band of the $^5D_0 \rightarrow {}^7F_0$ transition shifts to the lower energy side as the TiO_2 concentration increases, indicating the formation of Eu^{3+}−O^{2-}−Ti^{4+} bonding. At the same time, the emission intensity and the average decay time increase, revealing that the incorporation of TiO_2 can reduce the extent of the Eu^{3+} clusters. Fluorescence line-narrowing spectra indicate that the Eu^{3+} ions have two different environments, one of which exhibits a line-narrowing effect. The second-order crystal-field parameters show that the coordinating oxygen ions of site II are closer to the Eu^{3+} ions at the higher excitation energy. The analysis on the local structure of the Eu^{3+} ions suggests that the Ti^{4+} ions at site I occupy tetrahedral sites within the silica network, while some Ti^{4+} ions at site II occupy octahedral sites. The temperature dependence of the excitation spectra confirms that the $^7F_1$ level can be thermally populated in part and lower energy photons via thermally excited Eu^{3+} ions can make some electrons populate the $^5D_0$ level.

1. Introduction

In recent years, the optical properties of rare earth ions in sol−gel glasses have attracted considerable interest because of their potential applications as laser materials, sensors, high-density frequency-domain optical memory, and amplifiers for fiber-optic communication.[1−3] The sol−gel process provides a convenient method for preparing optical glasses due to the easily obtained different compositions and the ability to systematically study relationships among glass composition, structure, and optical properties of rare earth ions. Therefore, the optical properties of rare earth ions and several metal ions such as B^{3+}, Al^{3+}, Sn^{4+}, and P^{5+} ions incorporated into sol−gel silica glasses have been extensively investigated.[3−7] However, sol−gel glasses based on silica codoped with rare earth ions and Ti^{4+} ions have been paid little attention. On the other hand, TiO_2−SiO_2 mixed oxide materials have received considerable attention because of their interesting properties such as good chemical stability, low thermal expansion coefficient, and high refractive index that lead to their potential application in optoelectronic devices.[8,9] It is thus of significance to study the optical properties and local structure of the Eu^{3+} ions in TiO_2−SiO_2 glasses.

In this paper, we concentrated our attention on the optical properties and local structure of the Eu^{3+} ions in the TiO_2−SiO_2 glasses to explore the relationships among glass composition, local structure, and optical properties of the Eu^{3+} ions. At the same time, it was observed for the first time that there is an energy transfer from the O−Ti charge-transfer band to the Eu^{3+} ion in glasses and a population of the electrons in the $^7F_1$ level of the Eu^{3+} ions from room temperature to 8 K.

2. Experimental Section

2.1. Sample Preparation. The sample with the composition $x$$TiO_2$−(100 − x)SiO_2 containing 1% Eu_2O_3 was prepared by the sol−gel process with tetraethoxysilane (TEOS), ethanol, deionized water, $Ti(OC_4H_9)_4$, and $EuCl_3 \cdot 6H_2O$ as the starting materials. A small amount of concentrated hydrochloric acid was added as a catalyst. The $Si(OC_2H_5)_4$ was first hydrolyzed with a mixed solution of ethanol and deionized water. $Ti(OC_4H_9)_4$ was then introduced into the partially hydrolyzed TEOS solution, followed by stirring for 1 h at about 70 °C. When the solution was cooled to room temperature, $EuCl_3 \cdot 6H_2O$ dissolved in C_2H_5OH was added to this solution and stirred for 30 min. After this period, the mixed solution of H_2O and C_2H_5OH was added and the resultant solution was stirred for another 30 min to form homogeneous solution. The obtained homogeneous solutions were cast into plastic containers where they were allowed to gel at room temperature. Gel times varied from 4 to 8 weeks depending on the composition and room temperature. The final gel was heated at 500 °C in air for 4 h. The obtained samples are transparent and colorless. X-ray diffraction spectra of the samples are typical of amorphous glasses with no crystalline particle structure.

2.2. Characterization. The excitation and emission spectra were recorded at room temperature, using a monochromator (Jobin Yvon, HR 320) and a photomultiplier (Hamamatsu, R955). A 500-W xenon lamp with light that passed through a monochromator (Jobin Yvon, H 20) was used as the excitation source.

Decay curves were measured by an image-intensified charge coupled device (ICCD) system (Oriel Instruments, InstaSpec V) combined with a monochromator (Jobin, HR-320). A N_2 laser (λ_{ex} = 337.1 nm, pulse width <1 ns) was used as the excitation source. Fluorescence decays were monitored at the $^5D_0 \rightarrow {}^7F_2$ emission.

The $^7F_{0,1} \rightarrow {}^5D_0$ excitation and fluorescence line-narrowing (FLN) spectra were performed with the Jobin Yvon HR 320 monochromator. A tunable dye laser (Rhodamine 6G: 566−640 nm) pumped by an Ar^+ laser (Coherent, Innova 70) was used as the excitation source. The laser line width was ∼1.0

* Address correspondence to this author. E-mail: nogami@mse.nitech.ac.jp.

10.1021/jp0486245 CCC: $27.50
Published on Web 07/09/2004

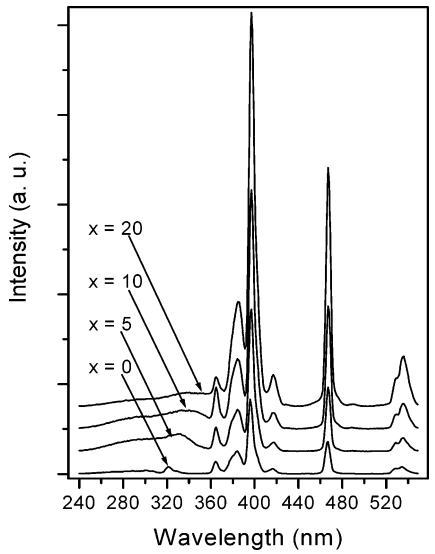

Figure 1. Excitation spectra of the Eu^{3+} ions in $x TiO_2-(100-x)SiO_2$ glasses ($\lambda_{em} = 614$ nm).

cm^{-1}. A chopper alternately opened the optical paths before and after the sample. The chopping frequency was 150 Hz. The $^7F_{0,1} \rightarrow {}^5D_0$ excitation spectra were measured by scanning the output of the dye laser and monitoring the $^5D_0 \rightarrow {}^7F_2$ emission. The FLN spectra were obtained by exciting the $^7F_0 \rightarrow {}^5D_0$ transition.

3. Results and Discussion

3.1. Excitation and Emission Spectra of the Eu^{3+} Ions in $xTiO_2-(100-x)SiO_2$ Glasses. Figure 1 shows the excitation spectra of the Eu^{3+} ions in $xTiO_2-(100-x)SiO_2$ glasses. The excitation spectrum of the Eu^{3+} ions in $100SiO_2$ glass consists of a broad band and several narrow bands. The broad band in the range from 240 to 310 nm is due to the charge-transfer band of the Eu^{3+} ion. The narrow bands at about 322, 364, 385, 396, 416, 467, and 536 nm are attributed to the f−f transitions within the Eu^{3+} $4f^6$ configuration.

In contrast to the excitation spectrum of the Eu^{3+} ions in pure SiO_2 glass, the excitation spectra of the Eu^{3+} ions in TiO_2-SiO_2 glasses exhibit two major changes associated with the increasing TiO_2 concentration. First, the excitation intensity of the f−f transitions increases, indicating that the Eu^{3+} surroundings have been changed. Second, a new band appears in the range from 310 to 360 nm and the position of the new band shifts to the lower energy side with the increasing TiO_2 concentration. A previous report[10] on the TiO_2:Eu thin film has shown that there is an energy transfer from the O−Ti charge-transfer band to the Eu^{3+} ions, which leads to the absorption of the O−Ti charge-transfer band in the similar range. Therefore, the new band is due to the O−Ti charge-transfer band. This result reveals that there is an energy transfer from the O−Ti charge-transfer band to the Eu^{3+} ions in the TiO_2-SiO_2 glasses. This observation provides a new red glass phosphor with a large excitation range.

Figure 2 shows the emission spectra of the Eu^{3+} ions in $xTiO_2-(100-x)SiO_2$ glasses. The emission spectra consist of five groups of emission bands at about 579, 582, 614, 653, and 702 nm. The five groups are due to the transitions from $^5D_0$ to ^7F_J ($J = 0,1, 2, 3, 4$), respectively.[10,11] In all cases only emission from the $^5D_0$ level was observed, revealing that the high-energy lattice phonons make the multiphonon relaxation process predominant between the ^5D_J levels. It can be seen from Figure 2 that the intensity of the Eu^{3+} emission increases with TiO_2 concentration. This result indicates the incorporation of titanium leads to an improvement of the Eu^{3+} surroundings. As a result, more efficient luminescent centers were formed. Previous investigations[2] on the rare earth ions in sol−gel silica glasses have shown that the rare earth ions have a tendency to form clusters. The cluster of rare earth ions is undesirable in most optical materials due to enhanced concentration quenching. The fact that the incorporation of TiO_2 results in an increase of the Eu^{3+} emission intensity suggests that the titanium ion can reduce the extent of the Eu^{3+} clusters. Therefore, TiO_2 plays a crucial role in the formation of efficient luminescent centers in the TiO_2-SiO_2 glasses.

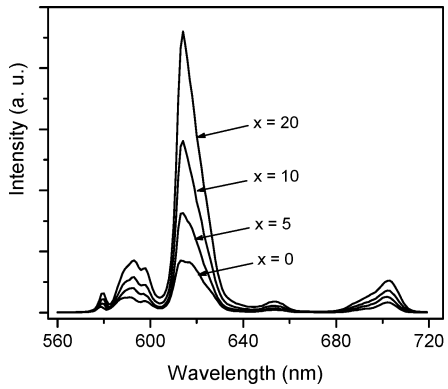

Figure 2. Emission spectra of the Eu^{3+} ions in $xTiO_2-(100-x)SiO_2$ glasses ($\lambda_{ex} = 396$ nm).

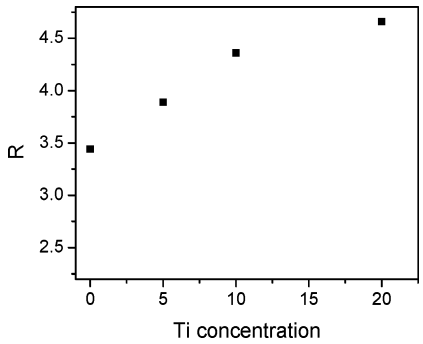

Figure 3. The intensity ratio of $^5D_0 \rightarrow {}^7F_2$ to $^5D_0 \rightarrow {}^7F_1$ of the Eu^{3+} ions as a function of Ti concentration in the $xTiO_2-(100-x)SiO_2$ glasses.

$^5D_0 \rightarrow {}^7F_2$ is an electric dipole allowed transition and its intensity is hypersensitive to the variation of the bonding environment of the Eu^{3+} ions, while $^5D_0 \rightarrow {}^7F_1$ is a magnetic dipole allowed transition and its intensity hardly varies with the bonding environment of the Eu^{3+} ions. The intensity ratio (R) of $^5D_0 \rightarrow {}^7F_2$ to $^5D_0 \rightarrow {}^7F_1$ increases as the degree of Eu−O covalence increases. Thus, the intensity ratio is widely used to investigate the bonding environment of the Eu^{3+} ions. The integrated intensity ratios of $^5D_0 \rightarrow {}^7F_2$ to $^5D_0 \rightarrow {}^7F_1$ of the different compositions are shown in Figure 3. Note that the integrated intensity ratio increases with TiO_2 concentration, indicating that the covalence degree of the Eu^{3+} ion increases. Considering the bonding structure of $Eu^{3+}-O^{2-}-Si^{4+}$ (or Ti^{4+}) and the fact that the Ti^{4+} ion has a larger radius and a smaller electronegativity, the increase of the covalence degree indicates the formation of $Eu^{3+}-O^{2-}-Ti^{4+}$ bonding.

The $^5D_0 \rightarrow {}^7F_0$ transition is also an effective probe of the bonding environment of the Eu^{3+} ions because there is no a crystal field splitting of the $^5D_0$ and $^7F_0$ levels. Therefore, the $^5D_0 \rightarrow {}^7F_0$ excitation and emission spectra also provide information on the covalence of the Eu^{3+} bonding. From the $^5D_0-{}^7F_0$ excitation (Figure 4) and emission (Figure 2) spectra, it can be

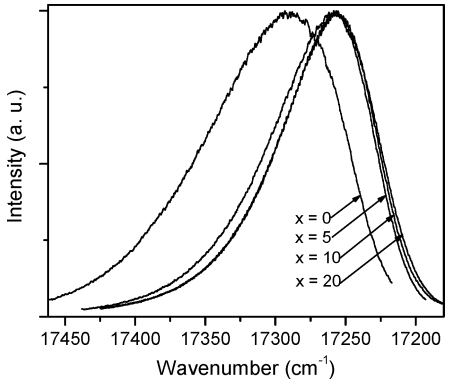

Figure 4. Excitation spectra of the $^5D_0-^7F_0$ transition in $x$$TiO_2$−(100 − x)SiO_2 glasses (λ_{em} =614 nm), measured at 8 K.

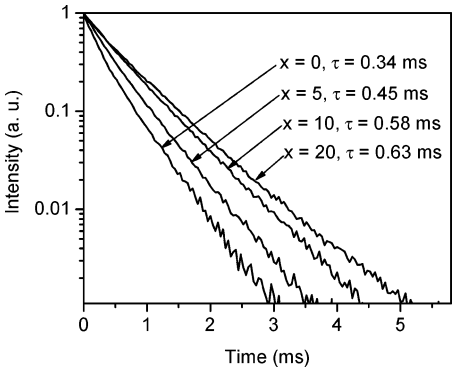

Figure 5. Normalized decay curves of the Eu^{3+} in $x$$TiO_2$−(100 − x)SiO_2 glasses. The excitation and monitoring wavelengths are 337.1 and 614 nm, respectively.

seen that the band of the $^5D_0\rightarrow{}^7F_0$ transition shifts to the lower energy side as the TiO_2 concentration increases. This result further indicates the covalence degree of the Eu^{3+} ions increases, revealing the formation of $Eu^{3+}-O^{2-}-Ti^{4+}$ bonding. Moreover, a smaller bandwidth of the $^5D_0\rightarrow{}^7F_0$ transition indicates that a narrower range of bonding environment is present for the Eu^{3+} ions in the TiO_2−SiO_2 glasses, suggesting the formation of $Eu^{3+}-O^{2-}-Ti^{4+}$ bonding leads to reducing the extent of the Eu^{3+} clusters. This suggestion is also supported by our experimental result on fluorescence decay time.

3.2. Fluorescence Decay Curves of the Eu^{3+} Ions in $x$$TiO_2$−(100 − x)SiO_2 Glasses. The fluorescence decay curve can offer the information on the change of the Eu^{3+} clusters because clustering of the Eu^{3+} ions leads to short $Eu^{3+}-Eu^{3+}$ distances, fast energy transfer, fluorescence quenching, and decay time shortening. A longer decay time means that the Eu^{3+} ions are better dispersed and less clustered.

Figure 5 shows the decay curves of the Eu^{3+} ions in $x$$TiO_2$−(100 − x)SiO_2 glasses. Note that the decay curves for all glasses under investigation deviated slightly from single exponentiality. The average decay times (τ) were determined from the decay curves. The average decay time is defined as the area under the normalized decay curve for each glass. For a pure exponential decay, the average decay time defined in this way is equal to the time constant of the decay. The obtained average decay times are also shown in Figure 5. It can be seen that the average decay time increases as the TiO_2 concentration increases from 0 to 20. This result further reveals that the incorporation of TiO_2 can reduce the extent of the Eu^{3+} clusters.

3.3. Fluorescence Line-Narrowing Spectra. The technique of laser-induced fluorescence line narrowing provides a microscopic probe of the local environment around the fluorescent

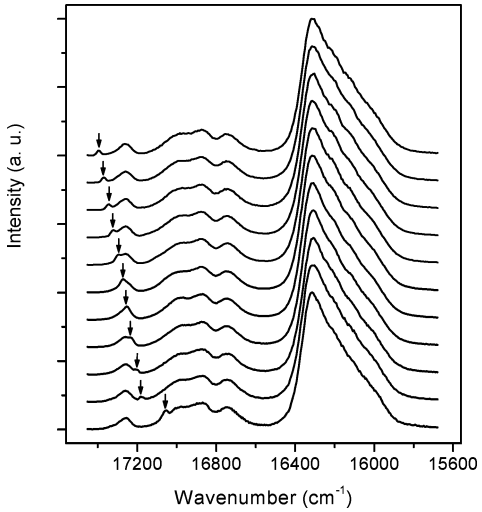

Figure 6. FLN spectra of the Eu^{3+} ions in $10TiO_2-90SiO_2$ glass, measured at 8 K. The arrows in the figure indicate the excitation position. Intensities are normalized to the most intense $^5D_0\rightarrow{}^7F_2$ transition peak.

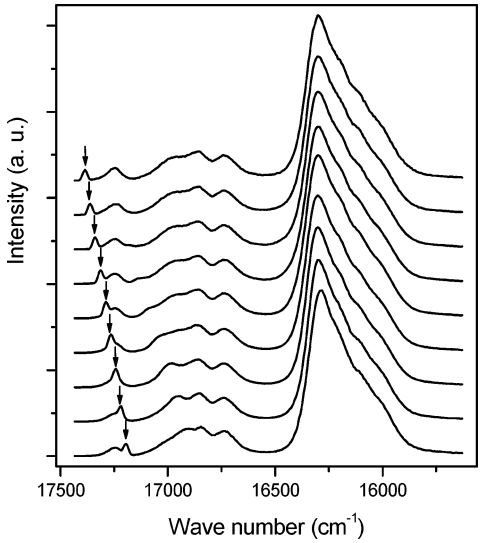

Figure 7. FLN spectra of the Eu^{3+} ions in $20TiO_2-80SiO_2$ glass, measured at 8 K. The arrows in the figure indicate the excitation position. Intensities are normalized to the most intense $^5D_0\rightarrow{}^7F_2$ transition peak.

ion. Crystal-field analyses of FLN spectra can provide insight into the local structure, while analysis of the variation in the spectra as a function of excitation wavelength can obtain the information on the distribution of sites in the glass. Therefore, FLN spectra are useful for studying the local structure around Eu^{3+} ions.

FLN spectra of $x$$TiO_2$−(100 − x)SiO_2 (x = 5, 10, 15 and 20) glasses were measured. The FLN spectra show similar properties when the TiO_2 concentration varied from 5 to 15; while the FLN spectrum shows some differences when the TiO_2 concentration is 20. The typical FLN spectra are shown in Figures 6 and 7. Three groups of lines, observed at 17354−17150, 17120−16580, and 16510−15730 cm^{-1}, are assigned to the $^5D_0\rightarrow{}^7F_0$, $^5D_0\rightarrow{}^7F_1$, and $^5D_0\rightarrow{}^7F_2$ transitions, respectively. It is interesting to note that the $^5D_0\rightarrow{}^7F_0$ emission can be observed even if the excitation energy is lower than that of the $^5D_0\rightarrow{}^7F_0$ energy gap. This observation suggests that the $^5D_0$ level can be populated by a low-energy photon and a thermally excited Eu^{3+} ion. This suggestion will be confirmed by

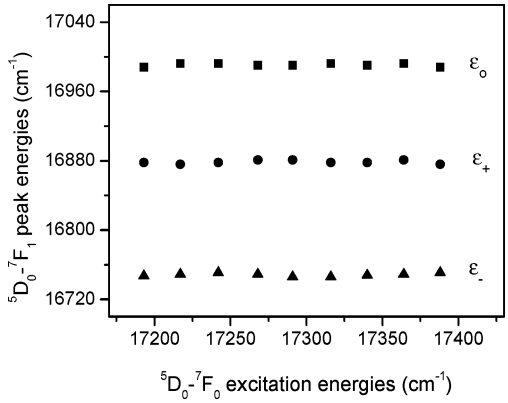

Figure 8. Peak energies of three $^5D_0 \rightarrow {}^7F_1$ fluorescence lines of the Eu^{3+} ions in $10TiO_2-90SiO_2$ glass as a function of $^7F_0 \rightarrow {}^5D_0$ excitation energy.

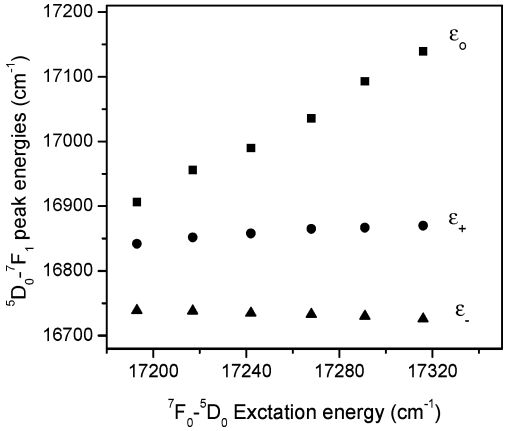

Figure 9. Peak energies of the three $^5D_0 \rightarrow {}^7F_1$ fluorescence lines of the Eu^{3+} ions in $20TiO_2-80SiO_2$ glass as a function of $^7F_0 \rightarrow {}^5D_0$ excitation energy.

examining the temperature dependence of the excitation spectra in section 3.4.

In the FLN spectra of $10TiO_2-90SiO_2$ glass, three distinct peaks in the range from 17156 to 16544 cm^{-1} are due to the Stark splitting of the $^7F_1$ level, indicating that the Eu^{3+} ions are located at one site (site I) with a symmetry of C_{2v} or lower. The shape and peak positions of the three components of the $^7F_1$ level appear to be independent of the excitation energy (Figure 8). No fluorescence line-narrowing effect was observed in the SiO_2-TiO_2 glasses within $15TiO_2$ concentration. This behavior is different from those observed in some other oxide glasses, where the three components of the $^7F_1$ level are shifted regularly with the excitation energy.[12−14] This behavior is similar to that observed in the silica glass containing Eu^{3+} ions, where the absence of the line-narrowing effect is due to the Eu^{3+} clustering that gives rise to an efficient energy transfer among Eu^{3+} ions.[15,16] Although some Si^{4+} ions are replaced by Ti^{4+} ions in the TiO_2-SiO_2 glasses, the network structure is very similar to that of silica glass. Therefore, it is suggested that the Eu^{3+} ions also have a tendency to form clustering although titanium ions can reduce the extent of the Eu^{3+} clusters. The absence of line-narrowing effect is also considered to be due to the Eu^{3+} clusters that lead to an efficient energy transfer among Eu^{3+} ions.

On the other hand, the FLN spectra of $80SiO_2-20TiO_2$ glasses show somewhat different behavior. In the FLN spectrum under 17388 cm^{-1} excitation, the $^5D_0 \rightarrow {}^7F_1$ transition was clearly split into three lines (16976, 16860, 16734 cm^{-1}). The positions of the three splitting lines remain unchanged with the increasing excitation energy. At the same time, a new emission line at ~17139 cm^{-1} was observed under 17316 cm^{-1} excitation. The energy and intensity of the new emission line gradually vary with excitation energy. Because the $^7F_1$ level in the crystal field is split into at most three levels at one site, the appearance of four peaks reveals that there are two sites for the Eu^{3+} ions in the $20TiO_2-80SiO_2$ glass.

On the basis of the spectral features of the different excitation energies, the $^5D_0 \rightarrow {}^7F_1$ transition bands of $20TiO_2-80SiO_2$ glass were separated into two groups. The behavior of one group is quite similar to that of $10TiO_2-90SiO_2$ glass, revealing that the Eu^{3+} ions have a similar bonding environment. The behavior of the other group (site II) shows a difference from that observed in $10TiO_2-90SiO_2$ glass, the energies of which are plotted in Figure 9 as a function of the excitation energy. It can be seen that the highest energy line gradually shifts to a higher energy side as the excitation energy increases, while the other two lines do not shift very much. The degree of the splitting of the $^7F_1$ level increases with the increasing excitation energy. This behavior of the Eu^{3+} ions at site II is quite similar to those of the Eu^{3+} ions doped oxide glasses,[12,13] where the site symmetry of the Eu^{3+} ions is considered to be C_{2v}, C_2, or C_s. On this basis, we assume that the site symmetry of the Eu^{3+} ions at site II is C_{2v}, C_2, or C_s.

To further investigate the variation in the local structure of the Eu^{3+} ions in the glass, the second-order crystal parameters of the Eu^{3+} ions at sites I and II should be considered. Since site I shows no line-narrowing effect, only the second-order crystal parameters of site II were considered. At first, the $M_{J=0}$ component ($E(\epsilon_0)$) should be determined. This component is nondegenerate in all axial symmetries and does not mix with the others until all symmetries are removed. This fact should be reflected by the luminescent behavior of the $^5D_0-{}^7F_1$ transitions. In the case of the Eu^{3+} ions at site II, the highest energy emission line of the three shifts much more than any other line and it is determined to be the $M_{J=0}$ component ($E(\epsilon_0)$). The other two emission lines therefore belong to the $E(\epsilon_-)$ and $E(\epsilon_+)$ components although the ordering remains ambiguous. Under these conditions, the second-order crystal parameters, B_{20} and B_{22}, can be estimated from the energies of the three $^7F_1$ lines by the following formulas:[14,17]

$$E(\epsilon_0) = E_0(^7F_1) + \frac{B_{20}}{5} \quad (1)$$

$$E(\epsilon_+) = E_0(^7F_1) - \frac{B_{20}}{10} + \frac{\sqrt{6}B_{22}}{10} \quad (2)$$

$$E(\epsilon_-) = E_0(^7F_1) - \frac{B_{20}}{10} - \frac{\sqrt{6}B_{22}}{10} \quad (3)$$

where $E_0(^7F_1)$ is the center of gravity of the $^7F_1$ multiplet, and $E(\epsilon_+)$, $E(\epsilon_-)$, and $E(\epsilon_0)$ are the energies of the corresponding components. B_{20} and B_{22} as a function of the excitation energy of the $^5D_0 \rightarrow {}^7F_0$ transition are shown in Figure 10. It can be seen that site II shows that the absolute value of B_{20} markedly increases, while that of B_{22} slightly increases, with the increasing excitation energy.

The relationships between the second-order crystal parameters and the lattice are as follows:[12]

$$B_{20} \propto (3z^2 - r^2)/r^3$$

$$B_{22} \propto (x^2 - y^2)/r^3 \text{ or } 2xy/r^3$$

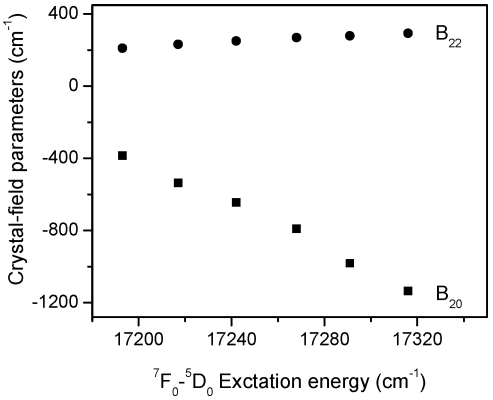

Figure 10. Second-order crystal-field parameters, B_{20} and B_{22}, of the Eu^{3+} ions in site II in the glass as a function of $^7F_0 \rightarrow {}^5D_0$ excitation energy.

The relations reveal that the variations in B_{20} and B_{22} come from the bonding environment of the Eu^{3+} ions. The increase in the absolute values of both B_{20} and B_{22} at site II with the excitation energy indicates that the coordinating oxygen ions are closer to the Eu^{3+} ions at higher excitation energy, implying that the coordinating oxygen ions are tightly bound and permitted less variation in the Eu^{3+} surroundings. This result reveals that there is a stronger crystal field in the Eu^{3+} surroundings, which leads to a larger splitting of the $^7F_1$ level. This result agrees with that of our experimental observation.

As the Eu^{3+} ion has been most often used as a microscopic probe of the local environment, similar properties of the FLN spectra reveal that the TiO_2−SiO_2 glasses within 15% TiO_2 concentration have a bonding environment similar to that of the Eu^{3+} ions, meaning that titanium ions are dissolved in the silica network and occupy tetrahedral sites. This result agrees with that of a previous investigation[8] on the structure of TiO_2−SiO_2 glasses, which suggested that the upper limit for solubility of TiO_2 in SiO_2 glass is ∼15 mol % and titanium ions occupy tetrahedral sites within the silica network. Considering the formation of Eu^{3+}−O^{2-}−Ti^{4+} bonding in the TiO_2−SiO_2 glasses, it is suggested that the Ti^{4+} ions in the bonding environment of the Eu^{3+} ions at site I occupy tetrahedral sites within the silica network. On the other hand, the appearance of the line-narrowing effect of the Eu^{3+} ions at site II reveals that the bonding environment of the Eu^{3+} ions differs from that of the Eu^{3+} ions at site I, while the difference in the bonding environment of the Eu^{3+} ions is associated with the variation of TiO_2 concentration. At higher TiO_2 concentration, some titanium ions act as network modifiers and occupy octahedral sites in the TiO_2−SiO_2 glasses.[8] These facts suggest that some Ti^{4+} ions in the bonding environment of the Eu^{3+} ions at site II occupy octahedral sites in the $20TiO_2$−$80SiO_2$ glasses.

3.4. Population of the Electrons in the $^7F_0$ and $^7F_1$ Levels of the Eu^{3+} Ions. The investigation of the population of the electrons in the $^7F_0$ and $^7F_1$ levels of the Eu^{3+} ions was paid little attention although the excitation spectra of the Eu^{3+} ions have been widely reported. However, this investigation can provide information on the detailed excitation and emission process. It is believed that information on the population of the electrons in the $^7F_0$ and $^7F_1$ levels can be obtained by measuring the excitation spectra associated with the $^7F_0$ and $^7F_1$ levels. Therefore, the excitation spectra of the Eu^{3+} ions in $10TiO_2$−$90SiO_2$ glass were measured at different temperatures and are shown in Figure 11. At room temperature, the excitation spectrum consists of four bands. The band at the high-energy side is due to the absorption from the $^7F_0$ level to the $^5D_0$ level.

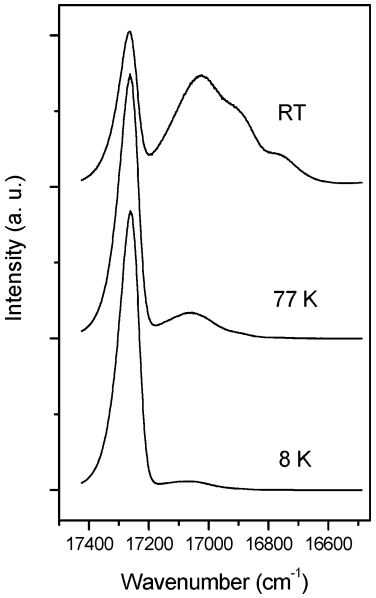

Figure 11. Excitation of the Eu^{3+} ions in $10TiO_2$−$90SiO_2$ glass at different temperatures (λ_{em} = 614 nm).

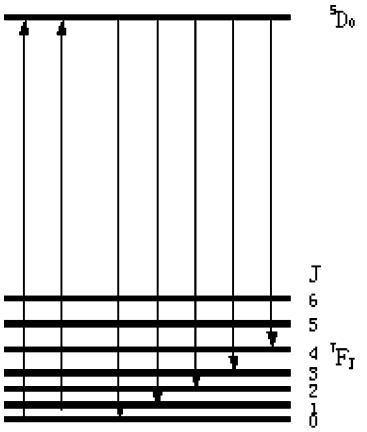

Figure 12. Excitation and emission processes of FLN spectra of the Eu^{3+} ions.

The other three bands at the low-energy side are assigned to the absorption from the three sublevels of the $^7F_1$ level to the $^5D_0$ level. This result reveals that the electrons at room temperature can populate both the $^7F_0$ and $^7F_1$ levels. As the temperature decreases, the absorption of the $^7F_0 \rightarrow {}^5D_0$ transition increases, while the absorption of the $^7F_1 \rightarrow {}^5D_0$ transition decreases, meaning that the population of the electrons in the $^7F_0$ level increases, while the population of the electrons in the $^7F_1$ level decreases. This phenomenon is due to the thermal population of the electrons. Because the $^7F_1$ level is higher than the $^7F_0$ ground level, the population of the electrons in the $^7F_1$ level requires higher phonon energy, compared with that of the electrons in the $^7F_0$ ground level, while phonon energy decreases as the temperature decreases. Therefore, the population of the electrons in the $^7F_1$ level decreases as the temperature decreases. This explanation agrees with the fact that the excitation spectra of the $^7F_0 \rightarrow {}^5D_0$ and $^7F_1 \rightarrow {}^5D_0$ transitions vary with the temperature. It is also noted that the $^7F_1$ level has some population even if the temperature is about 8 K. This result together with the fact that FLN spectra under the $^7F_1 \rightarrow {}^5D_0$ and $^7F_1 \rightarrow {}^5D_0$ transition excitations (Figure 6) appear in the $^5D_0 \rightarrow {}^7F_0$, $^5D_0 \rightarrow {}^7F_1$, and $^5D_0 \rightarrow {}^7F_2$ emission bands confirm that the $^5D_0$ emission level can be populated by a low-energy photon and a thermally

excited Eu^{3+} ion whose electron populates at the $^7F_0$ or $^7F_1$ level. This process is presented in Figure 12.

4. Conclusion

In this study, the optical properties of the Eu^{3+} ions in the sol−gel TiO_2-SiO_2 glasses were investigated. The appearance of the absorption of the O−Ti charge-transfer band in excitation spectra reveals there is an energy transfer from the O−Ti charge-transfer band to the Eu^{3+} ions. The increase of the covalence of the Eu^{3+} ion indicates the formation of Eu−O−Ti bonding. The average decay time increases as the TiO_2 concentration increases, indicating that the incorporation of TiO_2 can reduce the extent of the Eu^{3+} clusters. The FLN spectra exhibit that Eu^{3+} ions have two sites, one of which exhibits a line-narrowing effect. The second-order crystal-field analysis of the $^7F_1$ Stark splitting reveals that the coordinating oxygen ions of site II are closer to the Eu^{3+} ions with the increasing excitation energy, meaning that there is a stronger crystal field in the Eu^{3+} surroundings, which leads to a larger splitting of the $^7F_1$ level. The variation of the FLN spectra with the composition of TiO_2-SiO_2 glasses reveals that titanium ions occupy tetrahedral sites within the silica network in the TiO_2-SiO_2 glasses within 15% TiO_2 concentration. On further increase of TiO_2 concentration, some titanium ions act as network modifiers and occupy octahedral sites, which lead to the formation of the Eu^{3+} ions in site II. These results exhibit a good relationship among glass composition, local structure, and luminescent properties of the Eu^{3+} ions. The temperature dependence of the excitation spectra reveals that the electrons can populate the $^7F_1$ levels due to the thermal excitation. This situation led to the population of the $^5D_0$ level when the energy of excited light is lower than that of the $^5D_0 \rightarrow {}^7F_0$ energy gap.

Acknowledgment. This research was partly supported by the NITECH 21st Century COE Program for Environment-Friendly Ceramics.

References and Notes

(1) Biswas, A.; Maciel, G. S.; Kapoor, R.; Friend, C. S.; Prasad, P. N. *Appl. Phys. Lett.* **2003**, *82*, 2389.
(2) Stone, B. T.; Costa, V. C.; Bray, K. L. *Chem. Mater*. **1997**, *9*, 2592 and references therein.
(3) Nagami, M.; Suzuki, K. *Adv. Mater*. **2002**, *14*, 923.
(4) Zhong, Y.; Wang, M.; Wu, D. *Mater. Lett.* **1998**, *35*, 144.
(5) Nogami, M.; Nagakura, T.; Hayakawa, T.; Sakai, T. *Chem. Mater*. **1998**, *10*, 3991.
(6) Nagami, M.; Ohno, A.; You, H. *Phys. Rev. B* **2004**, *68*, 104204.
(7) Nagami, M.; Suzuki, K. *J. Phys. Chem. B* **2002**, *106*, 5395.
(8) Pickup, D. M.; Mountjoy, G.; Wallidge, G. W.; Anderson, R.; Cole, J. M.; Newport, R. J.; Smith, M. E. *J. Mater. Chem*. **1999**, *9*, 1299.
(9) Song, C. F.; Li, M. K.; Yang, P.; Xu, D.; Yuan, D. R. *Thin Solid Films* **2002**, *413*, 155.
(10) Frindell, K. L.; Bartl, M. H.; Popitsch, A.; Stucky, G. D. *Angew Chem., Int. Ed.* **2002**, *41*, 959.
(11) Ovenstone, J.; Titler, P. J.; Withnall, R.; Silver, J. *J. Phys. Chem. B* **2001**, *105*, 7170.
(12) Belliveau, T. F.; Simkin, D. J. *J. Non-Crystal Solids* **1989**, *10*, 127.
(13) Nogami, M.; Umehara, N.; Ishikawa, T. *Phys. Rev. B* **1998**, *58*, 6166.
(14) Tanaka, M.; Nishimura, G.; Kushida, T. *Phys. Rev. B* **1994**, *49*, 16917.
(15) Nogami, M.; Abe, Y. *Appl. Phys. Lett.* **1997**, *71*, 3465.
(16) Costa, V. C.; Lochhead, M. J.; Bray, K. L. *Chem. Mater*. **1996**, *8*, 783.
(17) Nishimura, G.; Kushida, T. *Phys. Rev. B* **1988**, *37*, 9075.